Becoming symbiotic – the symbiont acquisition and the early development of bathymodiolin mussels

Maximilian Franke[1], Benedikt Geier[1], Jörg U. Hammel[2], Nicole Dubilier[1,3]* and Nikolaus Leisch[1]*

[1] Max Planck Institute for Marine Microbiology, Celsiusstr. 1, 28359 Bremen, Germany

[2] Helmholtz-Zentrum Geesthacht, Institute of Materials Research, Max-Planck-Str. 1, 21502 Geesthacht, Germany

[3] MARUM—Zentrum für Marine Umweltwissenschaften, University of Bremen, Leobener Str. 2, 28359 Bremen, Germany

* corresponding author: nleisch@mpi-bremen.de, ndubilie@mpi-bremen.de

Abstract

Symbiotic associations between animals and microorganisms are widespread and have a profound impact on the ecology, behaviour, physiology, and evolution of the host. Research on deep-sea mussels of the genus *Bathymodiolus* has revealed how chemosynthetic symbionts sustain their host with energy, allowing them to survive in the nutrient-poor environment of the deep ocean. However, to date, we know little about the initial symbiont colonization and how this is integrated into the early development of these mussels. Here we analysed the early developmental life stages of *B. azoricus, "B". childressi* and *B. puteoserpentis* and the changes that occur once the mussels are colonized by symbionts. We combined synchrotron-radiation based µCT, correlative light and electron microscopy and fluorescence in situ hybridization to show that the symbiont colonization started when the animal settled on the sea floor and began its metamorphosis into an adult animal. Furthermore, we observed aposymbiotic life stages with a fully developed digestive system which was streamlined after symbiont acquisition. This suggests that bathymodiolin mussels change their nutritional strategy from initial filter-feeding to relying on the energy provided by their symbionts. After ~35 years of research on bathymodiolin mussels, we are beginning to answer fundamental ecological questions concerning their life cycle and the establishment of symbiosis.

Bathymodiolus, larvae, aposymbiotic, morphology

Introduction

Symbiont–host interactions play a fundamental role in all domains of life and mutualistic relationships are found in nearly all animal phyla. Such a partnership can expand the metabolic capabilities of the animals and allow them to colonize otherwise inhospitable habitats [1]. A prime example are bathymodiolin mussels which occur worldwide at cold seeps and hot vents on the ocean floor. Mussels of the genus *Bathymodiolus* house mutualistic, chemosynthetic symbionts in their gills, in cells called bacteriocytes [2]. The bacteria provide their hosts with organic products from the oxidation of chemicals in the vent fluids and different mussel species can harbour intracellular methane-oxidizing (MOX) and/or sulphur-oxidizing (SOX) symbionts [3].

A key process in all these symbiotic associations is the transmission of symbionts from one generation to the next. Symbionts can be either transmitted vertically from mother to offspring, intimately tying them to the reproduction and development of their host. Alternatively, symbionts can be recruited each generation anew from the environment. This horizontal transmission necessitates finding and recognizing the symbiotic partner and implies two lifestyles for each partner, stemming from the need to survive initially alone before symbiosis is established. In many organisms that rely on horizontally transmitted symbionts, morphological and developmental changes occur as soon as the symbionts are acquired to accommodate the new partner [4]. This can range from tissue rearrangement, as in the squid-vibrio symbiosis [5], to the development of an entire new bacteria-housing organ, like that seen in the hydrothermal vent tubeworm *Riftia pachyptila* [6].

Although mussels of the genus *Bathymodiolus* have been studied for over 35 years, their symbiont transmission, colonization and the early host development is still poorly understood [7]. Phylogenetic analyses showed no evidence of co-speciation, the hallmark of strict vertical transmission, between host and the thiotrophic symbiont and therefore suggested that bathymodiolin symbionts are transmitted horizontally [8-12]. The earliest host life stages were characterized only at the whole-animal scale using microscopy [13, 14], and the late larval stages analysed with transmission electron microscopy and stable isotopes showed already a well-developed symbiotic habitus, indistinguishable from the adult animals [15].This leaves the questions, if horizontal transmission is the case for both symbionts, at which developmental stage the host acquires the symbionts and how it accommodates the symbionts throughout the development still unanswered.

In this study, we combined synchrotron-radiation based micro-computed tomography (µCT), correlative light (LM) and transmission electron microscopy (TEM) and fluorescence in situ hybridization (FISH) to analyse developmental stages from planktotrophic larvae [14, 16] to adults of two *Bathymodiolus* species from hydrothermal vents, *B. puteoserpentis* and *B. azoricus*, and one from cold seeps, "*B". childressi* (also referred to as *Gigantidas childressi* e.g. [17]), across the Atlantic and compared them to the extensively studied shallow water relative Mytilus edulis [18]. The names of their late larval stages have been used interchangeably in the past and we therefore will use the following definitions. The dataset used here starts with the last planktonic larval stage - the pediveliger. Once settled in a suitable habitat the animal initiates the metamorphosis from planktonic to benthic lifestyle and enters the plantigrade stage of development. While metamorphosing the plantigrade degrades the velum, the larval feeding and swimming organ and develops into a post-larva. During the post larval stage the animal secretes the adult shell and once the ventral groove of the gills is formed [19] it enters the juvenile stage. It finally turns into a mature adult once the gonads are developed [18]. We investigated the early life stages of three bathymodiolin species, identified in which life stage the symbiosis is initiated, and how the symbionts colonize the animal. Furthermore, we identified a post metamorphosis change of the digestive system which potentially is linked to the symbiont colonization.

Materials and Methods

Sampling and fixation

All specimens were collected using remotely operated vehicles: *B. puteoserpentis* during the Meteor cruise M126 in 2016 at the Semenov vent field, *B. azoricus* during the Meteor cruise M82-3 in 2010 at the Bubbylon vent side, and *"B". childressi* during the Nautilus cruise NA58 in 2015 at the Mississippi Canyon 853. Upon recovery, specimens were fixed for histology and FISH in 2% paraformaldehyde (PFA) in phosphate buffer saline (PBS), and for histology and TEM in 2.5% glutaraldehyde (GA) in PHEM buffer (piperazine-N, N′-bis , 4-(2-hydroxyethyl)-1-piperazineethanesulfonic acid, ethylene glycol-bis(β-aminoethyl ether and $MgCl_2$; [20]). After fixation, samples were stored in the corresponding buffers (PFA: ethanol/PBS; GA: PHEM).

For details of samples and fixation methods see Table S1 and Table S2.

Shell measurements

Mussels were photographed with a stereomicroscope (Nikon SMZ 25, Nikon Japan) equipped with a colour camera (Nikon Ds-Ri2, Nikon Japan) and the software NIS-Elements AR (Nikon Japan). Measurements were recorded according to Figure S1c (Table S2) and shell margin limits were identified by their unique coloration (Figure S1d).

Histological analysis

PFA-fixed samples were decalcified with Ethylenediaminetetraacetic acid (EDTA). For histological analysis, samples were post fixed with osmium tetroxide (OsO_4) and embedded in low-viscosity resin (Agar scientific, UK). 1.5-µm sections were cut with a microtome (Ultracut UC7 Leica Microsystem, Austria) and stained with 0.5% toluidine blue and 0.5% sodium tetraborate. For TEM, semi-thin sections were mounted on a resin block, ultra-thin (70 nm) sections were cut on a microtome (Ultracut UC7 Leica Microsystem, Austria) and mounted on formvar-coated slot grids (Agar Scientific, United Kingdom) [21]. Sections were contrasted with 0.5% aqueous uranyl acetate (Science Services, Germany) for 20 min and with 2% Reynold's lead citrate for 6 min. For details see supplementary methods.

Dope-FISH

PFA-fixed *B. puteoserpentis* were dehydrated, embedded in paraffin and sectioned at 5–10-µm section thickness on a Leica microtome RM2255 (Leica, Germany). Sections were de-waxed, rehydrated and air dried. Modified Dope-FISH [22] was performed using specific probes targeting the 16s ribosomal subunit for the SOX and MOX symbionts as well as a general probe targeting all bacteria (Table S3). For details see supplementary methods.

Microscopy

Light microscopy (LM) analyses were performed using a Zeiss Axioplan 2 (Zeiss, Germany) equipped with an automated stage, two cameras (Axio CAM MRm Zeiss and Axio CAM MRc5 Zeiss, Germany) and an Olympus BX61VS (Olympus, Tokyo, Japan) slide-scanner equipped with an automated stage and two cameras (Olympus XM10, Tokyo, Japan and Pike F-505C, Allied Vision Technologies GmbH, Stadtroda, Germany).

Fluorescence microscopy analyses were performed using an Olympus BX53 compound microscope (Olympus, Tokyo, Japan) equipped with an ORCA Flash 4.0 camera (Hamamatsu Photonics K.K, Hamamatsu, Japan) using a 40× semi-Apochromat and a 100× super-Apochromat oil-immersion objective and the software cellSens (Olympus, Tokyo, Japan), and a Zeiss LSM 780 confocal laser-scanning microscope (Carl Zeiss, Jena, Germany) equipped with an Airyscan detector (Carl Zeiss, Jena, Germany) using a 100× Plan-Apochromat oil-immersion objective and the Zen-Black software (Carl Zeiss, Jena, Germany). For details see supplementary methods.

Ultra-thin sections were imaged at 20–30 kV with a Quanta FEG 250 scanning electron microscope (FEI Company, USA) equipped with a STEM detector using the xT microscope control software ver. 6.2.6.3123.

µCT measurements

All datasets were recorded at the Deutsches Elektronen-Synchrotron using the P05 beamline of PETRA III, operated by the Helmholtz-Zentrum Geesthacht (Centre for Materials and Coastal Research in Hamburg, Germany [23]). The x-ray microtomography setup at 15–30 keV and 5× to 40× magnification was used to scan resin-embedded, OsO_4-contrasted samples with attenuation contrast and uncontrasted samples in PBS-filled capillaries [24], with propagation-based phase contrast. Scan parameters are summarized in Table S4. The tomography data were processed in Matlab. Custom scripts implementing a TIE phase-retrieval algorithm and a filtered back projection, implemented in the ASTRA toolbox, were used for the tomographic reconstruction [25-27]. µCT models were used as ground truth for the volume calculations and to measure sectioning-induced tissue compression, which was on average 7%.

Image processing and 3D visualization

Histograms and white balance of microscopy images were adjusted using Fiji ver. V1.52p and Adobe Photoshop CS5 and figure panels were composed using Adobe Illustrator CS5 (Adobe Systems Software Ireland Ltd.). LM-images were stitched and aligned with TrackEM2 [28] in Fiji ver. V1.52p.

Threshold-based and manual segmentation were used to generate 3D models from LM and µCT datasets from representative individuals in Amira 6.7.0 (ThermoFisher Scientific). Co-registration between µCT and LM datasets and between LM and TEM datasets was carried out in Amira (Handschuh, Baeumler [21]. For details see supplementary methods.

Results

Here we analysed developmental stages of three species of *Bathymodiolus* mussels from aposymbiotic pediveliger to symbiotic adults. We determined at which stage the symbionts colonized the host, host adaptations to the symbiotic lifestyle and changes in host organ development (Figure 1).

General specimen classification

All *Bathymodiolus* individuals for this study were collected from mussel beds at hot vents and cold seeps on the sea floor. We therefore have to assume that even the earliest stages recovered were at least in the process of settling. We recorded shell dimensions and developmental stages of 259 *Bathymodiolus* individuals from three species (129 *B. puteoserpentis,* 124 *B. azoricus* and 6 "*B". childressi;* Table S2). The specimens ranged from 370 µm to 4556 µm shell length (Table S5). The earliest developmental stages found were pediveliger larvae with shell lengths of 366 µm to 465 µm. However, the shell dimensions alone did not allow us to differentiate between pediveliger and plantigrade (Figure S1a and b). As the dissoconch, the adult shell, is not developed at these two stages, a detailed morphological approach was required to separate them. Furthermore, 58 pediveliger and plantigrade individuals overlapped in shell size with the smallest post-larva (Figure S1f).

Morphological characterization of *Bathymodiolus* developmental stages

B. puteoserpentis specimens showed the best morphological preservation and covered the most complete range of developmental stages. Therefore, we focussed our detailed morphological studies on *B. puteoserpentis,* and compared our findings with selected samples from *B. azoricus* and *"B". childressi* (Figure S2 and S3). In the following, we describe the shared morphological features of all three species, unless specified otherwise.

The earliest stage recovered was the aposymbiotic pediveliger stage. *Bathymodiolus* pediveligers were characterized by the presence of a velum, a fully developed digestive system including membrane-bound lipid inclusions, a foot with two pairs of retractor muscles and two gill 'baskets' (Table S6, Figure 1a and Video S1). The velum, which is the larval feeding and swimming organ, was connected to the oral labial

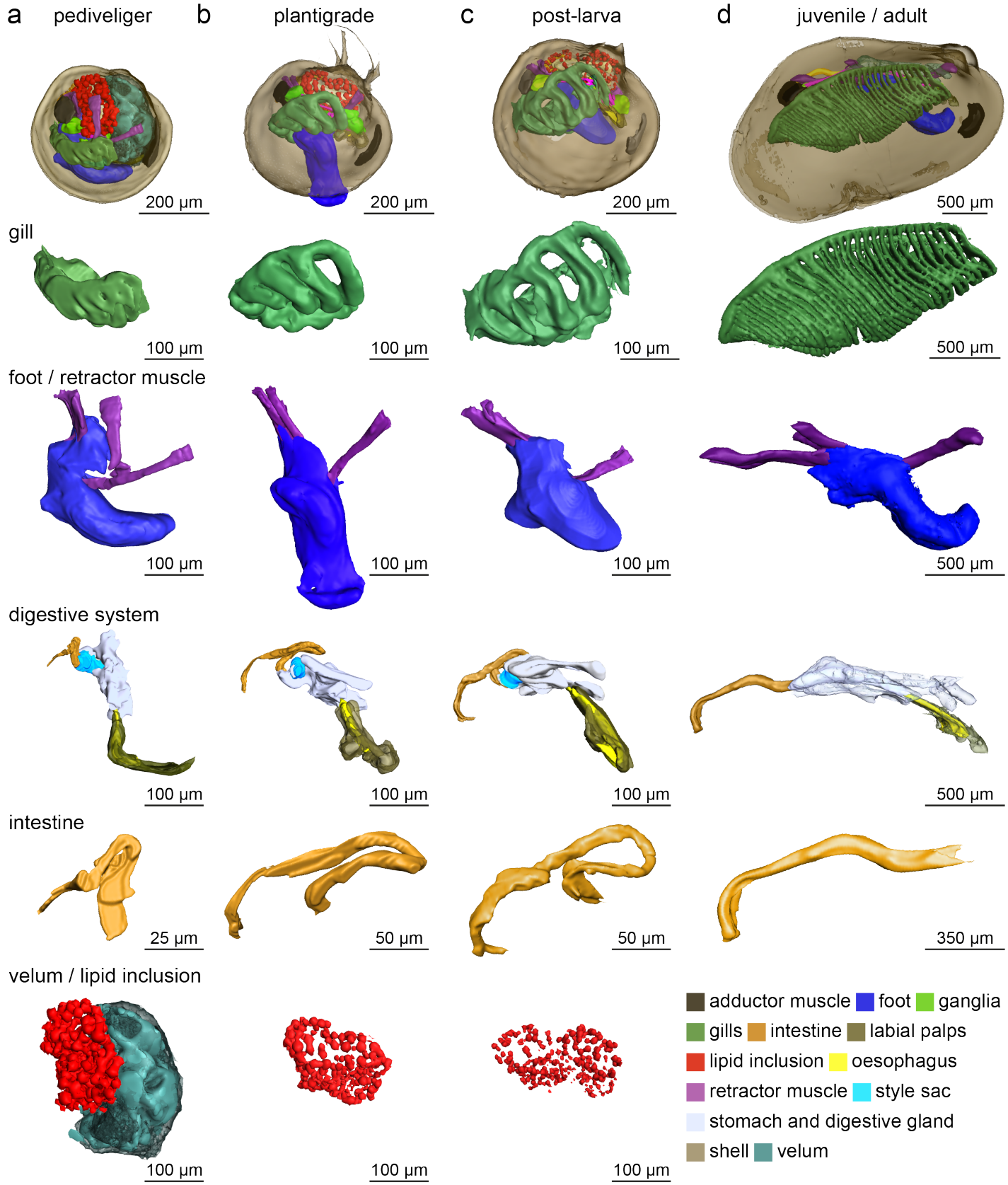

Figure 1 Three-dimensional visualization of individual organs during *B. puteoserpentis* development. Individual organs are displayed from the pediveliger (**a**), plantigrade (**b**), post-larva (**c**) and adult stage (**d**). Note the different scale bars in a–c and d. Three-dimensional data was obtained from section series and µCT measurements by threshold based and manual segmentation.

palp with a thin membrane (Figure S4 a and d). The digestive system consisted of the mouth, oral labial palp, oesophagus, stomach, two digestive glands, the style sac with crystalline style, the gastric shield, mid gut and an s-shaped looped intestine (Figure 1a and Figure S5).

The cells of the stomach contained membrane-bound lipid vesicles with an average diameter of 15.8 µm (n = 75; Figure 1 and Figure S5). *Bathymodiolus* pediveligers had a 'gill-basket' on each lateral side of the foot (Figure 1a and Figure S5). Each 'gill-basket' comprised three to four single gill filaments in *B. puteoserpentis* and five in *B. azoricus* and *"B". childressi* (Figure S2 b and c), which eventually form the descending lamella of the inner demibranch (Figure S5, Video S1). For further details, see supplementary Note 1.

In the plantigrade stage, the metamorphosis began with the degradation of the velum (Figure S4) and the appearance of byssus filaments (Figure S6). In this stage, rearrangements of all organs occurred, for example, the alignment of the growth axis of the gill 'basket' with the length axis of the mussel (Figure 1a-c, Figure S7 and Video S2). During metamorphosis, the number of gill filaments increased by one in all species (*B. puteoserpentis,* 5; *B. azoricus,* 6; and *"B". childressi,* 6; Figure S3). Furthermore, gill filaments separated from each other, increasing the gaps between them from 47 µm to 120 µm (Figure 1c). The change in gill morphology indicates a functional shift, from a purely respiratory organ to a filter feeding and respiratory organ. In the digestive tract, the number and volume of lipid vesicles decreased from 12.8% of the soft-body volume in pediveligers to 1.5% in post-metamorphosis mussels (mean diameter 8.37 µm, n = 60), and lipid vesicles were completely absent in juveniles and adults (Figure 1a-d and Table S6). In the last step of metamorphosis, the dissoconch was secreted and the mussels entered the post-larval developmental stage (Figure S1 and Figure S8). As the mussels transitioned from the post-larval to the juvenile stage, the digestive system straightened (Figure 1c-d, Figure S9 and Video S3 and S4). This morphological change was most prominent in the intestine, which changed from a looped to a straight shape and remained straight in all later developmental stages (Figure 1c-d and Figure S9). For further details see supplementary note 2.

Establishment of the symbiosis

Key to accurately assessing symbiont colonization and symbiont-mediated morphological changes was our use of a correlative µCT, light and electron microscopy approach (Video S5, Figure S10) complemented with FISH. This allowed us to rapidly screen whole animals, yet achieve the resolution necessary to identify single eukaryotic cells that were in the process of being colonized by the symbionts. Previous studies [12, 29] emphasized that in juvenile and adult *Bathymodiolus* mussels, colonized epithelia cells remodel their cell surface by losing their microvilli and cilia and show a swollen (hypertrophic) habitus compared to non-colonized epithelia cells (Figure 2 c, f and i). We tested whether this morphological change is detectable in the LM dataset and has predictive power for symbiont colonization. Scoring 1813 epithelia cells from six individuals in both the LM and the correlative TEM datasets (average cell count per sample 302) showed that all cells predicted to be colonized on the basis of morphology in the LM dataset were indeed colonized by symbionts in the TEM dataset, and likewise, all cells predicted to be aposymbiotic on the basis of morphology were free of symbionts (Figure S10). In the pediveliger stage, none of the epithelial cells were colonized by symbionts (n = 797 host cells in 2 pediveliger). In the plantigrade stage 15% (n = 336 host cells in 1 plantigrade) and in the post-larval stage 23% (n = 680 host cells in 3 post larvae) of all analysed gill, mantle, foot and retractor muscle epithelia cells were colonized by symbionts. Informed by the correlative imaging approach, we were able to identify individual MOX symbionts in the light microscopy images (Figure S10).

Our correlative approach allowed us to analyse whole animal datasets to identify host cells that were in the process of being colonized, with the goal of determining the timing of symbiont uptake in *Bathymodiolus* mussels (video S5). The pediveligers of all three analysed bathymodiolin species were aposymbiotic and the epithelial cells of all tissues were ciliated and had microvilli (Figure 2 a, d and g). However, two of the aposymbiotic pediveligers had bacterial morphotypes similar to the symbionts attached to the outside of their shell (Figure S11). Expanding our analyses to all three host species showed that the smallest mussels with symbionts were plantigrades of *B. puteoserpentis* with a shell length of 432 µm, *B. azoricus* with a shell length of 510 µm and *"B". childressi* with a shell length of 383 µm. In these plantigrade stages, we observed symbionts in epithelial cells of the gill filaments, mantle, foot and retractor muscle (Figure 2 b, e, h and j–m). We analysed multiple developmental stages and observed that as soon as the symbionts colonized an epithelial cell, the cilia and microvilli of the host cell were no longer visible (Figure 2 h) and the cells had a hypertrophic morphology (Figure 2b-c, e-f, h-i). Following symbiont colonization, the gill tissue showed the colonization pattern known from adult animals: the majority of cells were bacteriocytes, and only intercalary cells, cells at the ventral ends of the gill filaments, and those at the frontal-to-lateral zones along the length of the filaments were aposymbiotic, remained ciliated and had microvilli (Figure S7, S8 and S10). In the post-larval, juvenile, and early adult stages, in all of the three analysed species, the epithelia of the gill, mantle, foot and retractor muscles were fully colonized by their corresponding symbiont type (Figure 2 c, f and i) (*B. puteoserpentis* and *B. azoricus,* SOX and MOX symbionts; *"B". childressi,* MOX symbionts).

We were also able to analyse the dynamics of colonization in in *B. puteoserpentis.* Symbiont colonization started with only a few bacterial cells in the plantigrade stage (Figure 2b, e, f, j-m) and bacterial density per host cell (Table S7) was the lowest, but steadily increased in the later developmental stages, reaching up to 120 symbionts per gill bacteriocyte in the post-larval stage. With the onset of symbiont colonization, the phagolysosomal digestion of the symbionts by the host could be detected (Figure 2 b – c and e – f).

The process of symbiont colonization seemed to be rapid. Most individuals had either no tissue at all or all their epithelial tissues colonized. Only in two out of 15 *B. puteoserpentis* individuals we could observe bacterial morphotypes of SOX and MOX symbionts that were not yet completely engulfed by the host's cell membrane, which we interpreted as ongoing tissue colonization (Figure 2 j – m). This was particularly prominent in mantle epithelia cells, while in the same specimens the gill epithelial cells were already fully colonized (Figure 2b, e and f). Furthermore, we observed mantle and foot cells that were colonized by SOX and MOX symbionts (Figure 2 h) and cells colonized only by SOX symbionts (Figure 2 e), but we never observed cells which were only colonized by MOX symbionts. Despite using a eubacterial FISH probe and analysing sections via TEM we never observed bacterial morpho- or phylotypes other than SOX and MOX symbionts (Figure 2, Figure 3, Figure S12 and Figure S13).

Discussion

Post-metamorphosis development deviates from the mytilid blueprint

We compared the early development of the three analysed *Bathymodiolus* species with the well-studied non-symbiotic shallow-water relative *Mytilus edulis* [18, 19]. In doing so we detected an overlap in size of 50 µm in shell length between *Bathymodiolus* pediveliger and plantigrade, and between plantigrade and post-larva. Even though shell dimensions were previously used to determine the developmental stage of bivalves, our work shows that alone, they are not a reliable indicator.

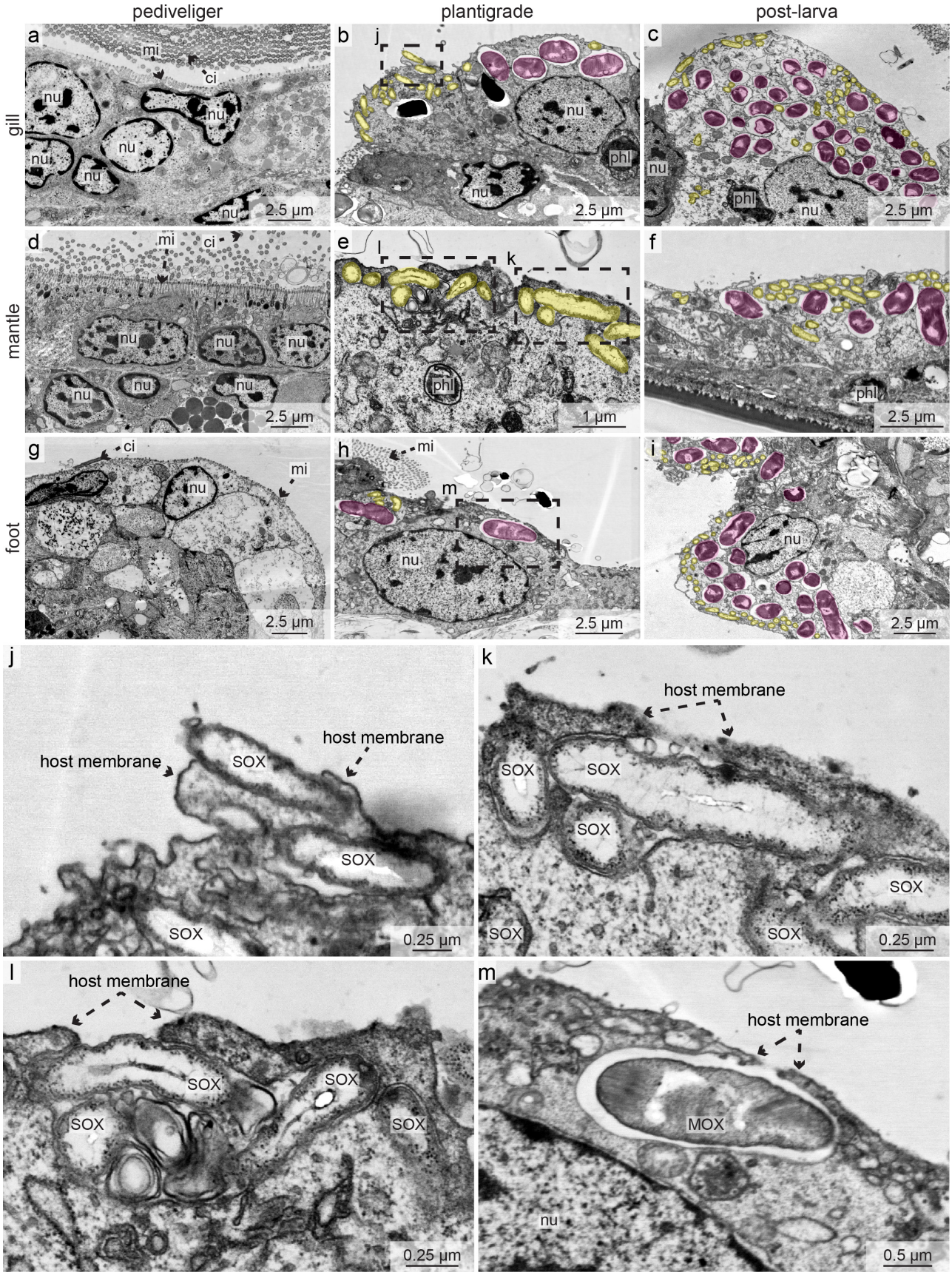

Figure 2 Symbiont colonization starts during the plantigrade stage in *Bathymodiolus puteoserpentis*. TEM micrographs of different epithelial tissues and their state of symbiont colonization: gills (a–c), mantle (d–f) and foot (g–i) of individuals at the pediveliger (a, d and g), plantigrade (b, e and h) and post-larva stage (c, f and i). SOX (yellow) and MOX symbionts (magenta) are shown in false colours (a–i). For raw image data see supplement Figure S14. All epithelial tissues of the pediveliger stage are aposymbiotic (a, d and g). In the plantigrade stage, the colonization of both symbiont types is still ongoing (b, e and h). In the post-larva stage, all epithelial tissues are colonized by both symbiont types (c, f and i). Dashed boxes indicate regions in which symbionts are actively colonizing epithelial tissue (shown magnified in j – m). ci, cilia; mi, microvilli; MOX, methane-oxidizing symbiont; nu, nucleus; phl, phagolysosome; SOX, sulphur-oxidizing symbiont.

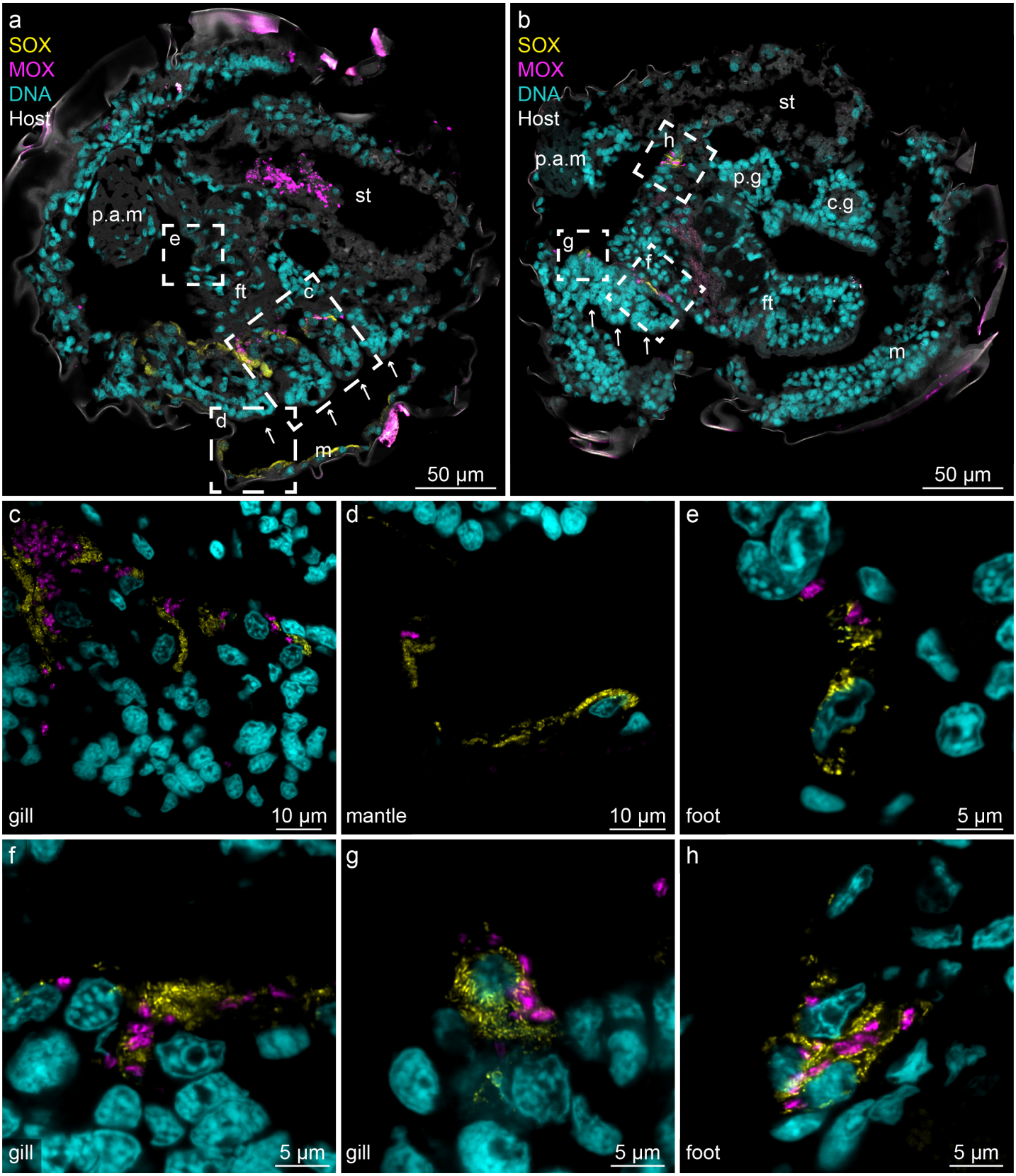

Figure 3 SOX and MOX symbionts colonize all epithelial tissues in *Bathymodiolus puteoserpentis* post-larvae. False-coloured FISH images show probes specific for SOX (yellow, BMARt-193) and MOX symbionts (magenta, BMARm-845) and host nuclei stained with DAPI (cyan). Sagittal cross sections of two different individuals (**a** and **b**) show SOX and MOX symbionts colonizing the gill, foot and mantle epithelia. To outline host tissue, autofluorescence is shown in white in **a** and **b.** Dashed boxes indicate magnified regions of the colonized gill, mantle and foot region shown in **c–h.** c.g, cerebral ganglion; ft, foot; p.a.m, m, mantle: posterior adductor muscle; p.g, pedal ganglion; st, stomach; →, gill filament.

The size overlap indicates that the initiation of metamorphosis is not size dependent and that mussels of the genus *Bathymodiolus* are able to delay their metamorphosis. Such a delay and continued growth could be due to a lack of settlement cues and/or limited nutrition, similar to what is known from *M. edulis* [30]. Delaying metamorphosis would favour dispersal, potentially leading to an increase in species distribution and the colonization of new habitats.

The pre-metamorphosis development of *Bathymodiolus* mussels is very similar to that of their shallow water relative *M. edulis* [18, 30]. The pediveliger of both *Bathymodiolus* and *Mytilus* develop a large velum, foot, mantle epithelium, digestive system, central nerve system and two preliminary gill baskets consisting of three to five gill buds [18]. During the metamorphosis of *Bathymodiolus* mussels, the velum is degraded, organs within the mantle cavity are rearranged and the lipid vesicles in the digestive tract are reduced. In early developmental stages of mussels of the families *Mytilidae* and *Teredinidae,* lipid vesicles serve as energy supply to sustain the energy intensive metamorphosis [18, 31], and they are likely to have a similar function in *Bathymodiolus.* Furthermore, these lipid vesicles could provide the energy to support the pediveliger stage moving between vent or seep sites [32, 33].

Although the early development appears to be conserved between *Bathymodiolus* mussels and their shallow water relatives, differences occur as soon as symbiont colonization begins. We observed striking morphological changes in epithelial tissues. The colonized cells lost both microvilli and cilia, and developed a hypertrophic (swollen compared to non-colonized epithelial cells) habitus, as previously documented for bacteriocytes of juveniles and adults [12, 29]. Remodelling of the cell surface and induction of the loss of cilia and microvilli has been reported for many bacteria e.g. pathogenic *Escherichia coli, Pseudomonas sp.* and *Vibrio sp.* that associate with a wide range of epithelia [34-36]. Our findings demonstrate that these cell surface modifications serve as reliable markers for the state of symbiont colonization for all epithelial tissues of early life stages.

After completion of metamorphosis, we observed a streamlining of the digestive system (Figure 4). The stomach and the intestine straightened and the digestive system changed from the complex looped type found in *Mytilus* [18] to the straight type seen in *Bathymodiolus* adults (Table S8, [37, 38]). Such change in morphology is striking, as in mytilids no further morphological changes occur after metamorphosis [18]. Conspicuously, in *Bathymodiolus* this morphological change follows the establishment of the nutritional symbiosis (Figure 4). We hypothesize that symbiont colonization initiates a shift in nutrition, which leads to the streamlining of the digestive system. In general, the morphology of the gastrointestinal tract reflects the chemistry of an organism's food sources. Organisms that digest complex foods possess enlarged compartments and gastrointestinal structures to slow down digesta flow to allow breakdown of complex molecules [39]. We

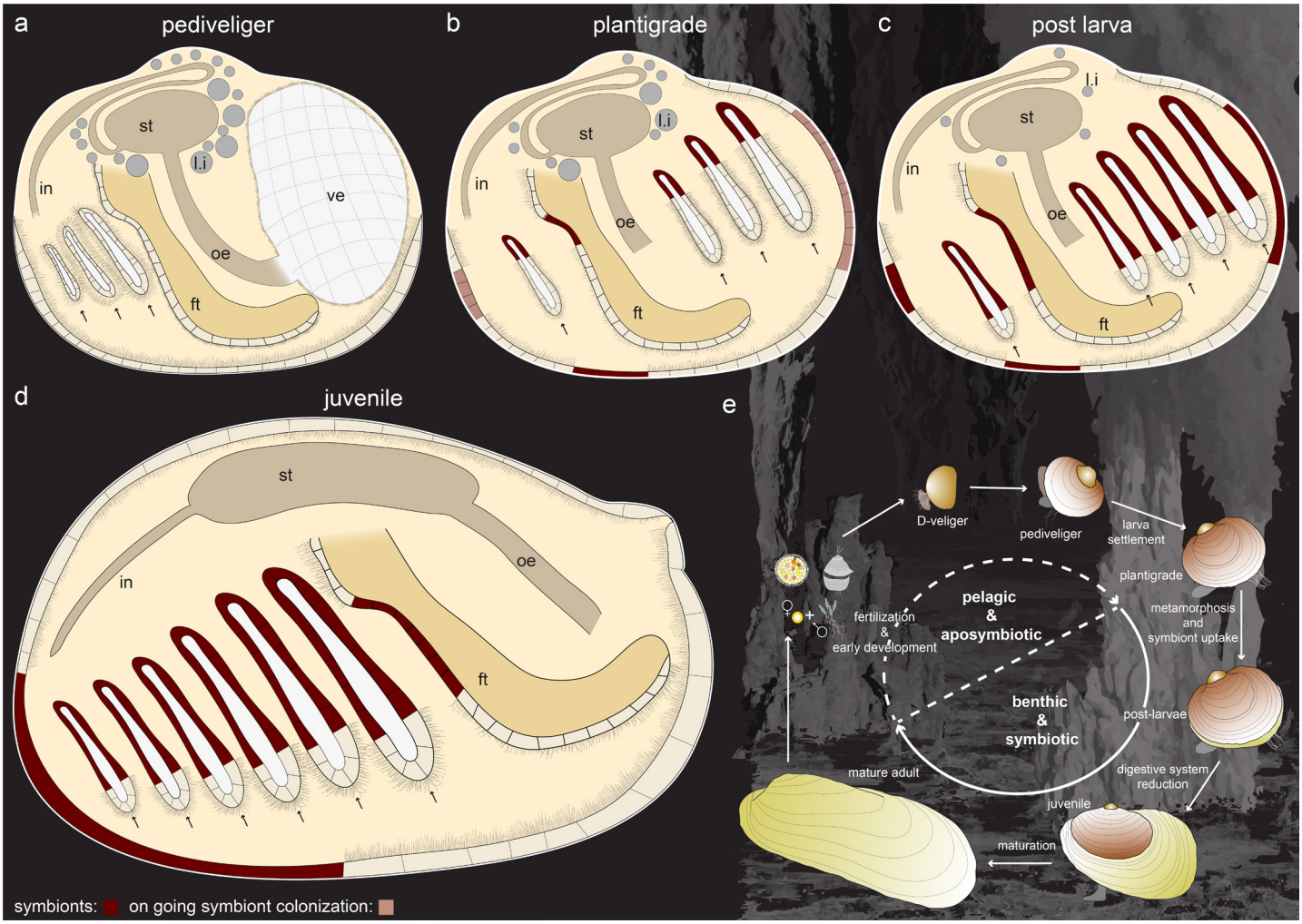

Figure 4 Summary of the development and symbiont colonization of bathymodiolin mussels. Pediveliger are aposymbiotic (a), and symbiont colonization starts during the plantigrade stage (b). By the post-larval (c) and juvenile (d) stages, all epithelial tissues have become colonized by symbionts. The digestive system is reduced between the post-larva and juvenile developmental stages, adopting a straight morphology. (e) Schematic of the hypothetical life cycle of bathymodiolin mussels indicating the aposymbiotic pelagic developmental stages and the symbiotic benthic developmental stages. ft, foot; in, intestine; l.i, lipid inclusion; oe, oesophagus; →, gill filament.

postulate that while *Bathymodiolus* larvae are aposymbiotic and rely on filter feeding, they require a complex intestine to digest a diverse diet. Once they shift from filter feeding to obtaining the majority of their nutrition from intracellular symbionts, the morphology of the digestive tract changes. It is interesting to note that adult bathymodiolin mussels of the closely-related genus *Vulcanidas* that occur in shallow waters close to the photic zone (140 m compared to 1000–3500 m depth for the samples studied here) have a pronounced looped intestine [40]. With more food input from the photic zone, filter feeding might play a greater role in nutrition for these *Vulcanidas* mussels. This raises the question whether streamlining of the digestive tract is a conserved developmental trait among *Bathymodiolus* species, or if the environment and access to external food sources dictates this post-metamorphosis development.

Symbiont colonization begins as soon as the velum is degraded during the plantigrade stage

The mode of symbiont transmission in mussels of the genus *Bathymodiolus* has been the focus of several studies. Ultrastructural analyses of the male and female gonads showed no evidence of symbionts associated with either egg or sperm [41, 42]. In the closely related "*Idas*" *simpsoni* mussel, light microscopy and DAPI-staining based analyses showed aposymbiotic animals until the juvenile stage [43]. Moreover, in *Bathymodiolus*, host and SOX symbiont phylogenies show no congruency – contrary to what would be expected under strict maternal transmission. These observations suggest that the mussels acquire their symbionts anew each generation [8-10]. However, as recently highlighted by Laming, Gaudron [7], how and when the mussels acquire their symbionts remained unclear. Here we not only show early developmental aposymbiotic stages, which must recruit symbionts from the environment, but also narrow the window of symbiont acquisition down to the latest stage of metamorphosis (Figure 4).

Our data suggest that symbionts can only reach the gills once the velum is lost. As long as the velum is present and active, particles are either transported directly into the digestive system or expelled from the mussel. During the development of *M. edulis*, once the velum is degraded the gill filaments move further apart and take over the task of sorting food particles and generating a water current [18, 19]. In the late plantigrade stage of *Bathymodiolus,* we identified a similar increase of space between the gill filaments. Only once the gills take over the function of particle sorting and water current generation, could a symbiont make physical contact with the gill epithelium and initiate colonization.

The initial symbiont colonization seems to be rapid, based on our assessment of 25 *Bathymodiolus* individuals. These individuals were either completely aposymbiotic or all their epithelial tissues were fully colonized, except for two individuals at the plantigrade stage in which we detected ongoing symbiont colonization. As we were working with preserved samples that represent a snapshot of development, the chance of observing a process depends on its frequency and length. The less frequent or the faster a process happens, the smaller the chance of observing it. As colonization occurs in all individuals, the infrequent observation of ongoing colonization would therefore suggest that colonization happens rapidly. This probably reflects the need of the mussels to quickly acquire symbionts once they have settled in such a nutrient-limited habitat. At this stage, energy reserves are used for the metamorphosis and the velum is broken down, which diminishes the filter feeding capabilities. Rapid symbiont colonization could be accommodated by a reservoir of free-living symbionts at these habitats or by specific recognition mechanisms, whereby, for example, the presence of the symbionts induces settlement and metamorphosis.

Although, *Bathymodiolus* pediveliger tissues were aposymbiotic, we could identify morphotypes similar to the known symbionts on the outside of the mussel shell. Such a biofilm on the shell could serve as a staging ground for later symbiont colonization. Recent work has highlighted how bacteria can induce settlement and metamorphosis in marine invertebrates [44]. In a similar manner, if the plantigrade stage of *Bathymodiolus* were to rely on bacterial cues to initiate settlement and metamorphosis, this would ensure that the symbiont could be taken up from the environment immediately following metamorphosis. As an additional benefit, this would increase the chances for the larva to take up locally adapted symbionts. The difference in vent fluid composition of hydrothermal vents can have a strong impact on the fitness of mussels [45]. Locally adapted symbionts would thus be highly beneficial to the symbiosis, and recent work showed that one mussel can even host multiple strains of SOX symbionts. These strains can differ in key functions, such as the use of energy and nutrient sources, electron acceptors and viral defence mechanisms [46]. By hosting multiple locally adapted symbiont strains the mussels are best adapted to the fluctuating vent conditions.

Symbiont colonization starts in the gills and proceeds to other epithelial tissues

In post-larvae and juveniles, the symbionts occur in epithelial cells of the gills, mantle, foot and retractor muscle [15, 47, 48]. Previous work suggested that the symbionts initially colonize the mantel tissue, which in mytilids develops earlier than the gill filaments, and from there bacteria spread into the epithelia cells of the gills and foot [15, 47]. The symbionts in foot and mantle tissue could provide an additional source of nutrition to post-larval and juvenile mussels [15, 48]. Our data show that four to five gill filaments formed before metamorphosis, when the animals were still aposymbiotic. Therefore, the proposed symbiont colonization via the mantle into the developing gill filaments is unlikely. Additionally, in two *B. puteoserpentis* specimens we detected fully colonized gills while the mantle tissue was in the process of being colonized. Taken together, our findings support a colonization route via the gills as the first point where symbiosis is established.

The process of symbiont colonization appears to be highly specific, as we never observed bacterial morpho- or phylotypes other than the known SOX and MOX symbionts associated with epithelia cells. This suggests a strong recognition mechanism on the side of either the symbiont or the host. In invertebrates, the innate immune system of the host plays a key role in the process of symbiont–host recognition and uptake [49]. For example, transcriptomic studies of *Bathymodiolus platifrons* have highlighted the presence and strong expression of gene families related to symbiont recognition, acquisition and maintenance [50-52]. In the case of *B. puteoserpentis,* it is tempting to speculate that the SOX symbiont pioneers tissue colonization, as we observed cells that were actively colonized by the SOX symbiont only, but never by MOX symbionts only. The SOX symbiont could have a priming effect, which allows the MOX symbiont to colonize later. Now that we have narrowed down the window of first contact and symbiont colonization, a spatial transcriptomic approach could shed light on the underlying molecular mechanism of host–symbiont recognition and subsequent colonization.

Conclusion

After 35 years of vtudy of bathymodiolin mussels, we are only now beginning to understand their lifecycle and the establishment of symbiosis. Our data not only identify aposymbiotic life stages, but also reveal the tight integration of symbiont uptake following loss of the velum and the high specificity of symbiont acquisition. Our correlative imaging workflow allowed us to carry out virtual dissection of this host–symbiont interaction from the subcellular to the whole animal

scale and to follow developmental changes throughout the lifecycle. This whole lifecycle approach is critical to differentiate the conserved developmental blueprint from specific developmental changes induced by associating with symbiotic microbes. This approach lends itself to the study of the early development of biological diversity more widely, especially in non-model systems or animals living in remote habitats or with limited sample availability. Moreover, the framework generated by this approach enables targeted genomic and transcriptomic studies. A morphology-informed dual RNA-seq approach that recovers both host and symbiont transcripts could be used to understand symbiont recognition, attachment, and colonization throughout the initial tissue colonization. Once integrated with morphological data, this would move us towards an in-depth understanding of the underlying molecular interactions and their effects on host–microbe systems.

Data accessibility

LM-data and µCT-data is available on figshare. The DOIs are listed in Table S1.

Supplementary videos are available with the following DOIs:
Video S1: https://doi.org/10.6084/m9.figshare.13049765.v2
Video S2: https://doi.org/10.6084/m9.figshare.13049807.v1
Video S3: https://doi.org/10.6084/m9.figshare.13049870.v1
Video S4: https://doi.org/10.6084/m9.figshare.13049882.v1
Video S5: https://doi.org/10.6084/m9.figshare.13049993.v1

Author contributions

M.F. planned the research, performed the light and fluorescence microscopy, analysed all light, TEM, fluorescence and µCT datasets, reconstructed all 3D models, designed all figures, produced all videos and wrote the manuscript. **B.G.** helped with the 3D reconstructions and µCT-measurements, and revised the manuscript. **J.U.H.** performed the µCT measurements with help from **B.G.** and **M.F.**, reconstructed all µCT-datasets and revised the manuscript. **N.D.** provided funding and revised the manuscript. **N.L.** planned the research, did the TEM re-sectioning, performed the TEM measurements and wrote the manuscript.

Competing interests

We declare no competing interests.

Funding

Funding was provided by the Max Planck Society, a Gordon and Betty Moore Foundation Marine Microbial Initiative Investigator Award (grant no. GBMF3811 to N.D.) and a European Research Council Advanced Grant (BathyBiome, Grant 340535 to Nicole Dubilier).

Acknowledgements

We thank the captains, crew members and ROV pilots of the cruises M126, M82-3 and NA58. Furthermore, we gratefully acknowledge W. Ruschmeier for her help in the lab. We would like to thank all those involved in supporting us at the Deutsches Elektronen-Synchrotron at the P05 beamline of PETRA III, operated by the Helmholtz-Zentrum Geesthacht (Centre for Materials and Coastal Research in Hamburg, Germany, proposal Ids: 20170337, 20180295).

References

[1] McFall-Ngai, M., Hadfield, M.G., Bosch, T.C.G., Carey, H.V., Domazet-Lošo, T., Douglas, A.E., Dubilier, N., Eberl, G., Fukami, T., Gilbert, S.F., et al. 2013 Animals in a bacterial world, a new imperative for the life sciences. Proceedings of the National Academy of Sciences **110**, 3229-3236. (doi:10.1073/pnas.1218525110).

[2] Dubilier, N., Bergin, C. & Lott, C. 2008 Symbiotic diversity in marine animals: the art of harnessing chemosynthesis. *Nature reviews. Microbiology* **6**, 725-740. (doi:10.1038/nrmicro1992).

[3] DeChaine, E. & Cavanaugh, C.M. 2005 Symbioses of methanotrophs and deep-sea mussels (*Mytilidae*: *Bathymodiolinae*). *Progress in Molecular and Subcellular Biology* **41**, 227-249. (doi:10.1007/3-540-28221-1_11).

[4] Bright, M. & Bulgheresi, S. 2010 A complex journey: transmission of microbial symbionts. *Nature reviews. Microbiology* **8**, 218-230. (doi:10.1038/nrmicro2262).

[5] McFall-Ngai, M.J. 2014 The importance of microbes in animal development: lessons from the squid-vibrio symbiosis. *Annual review of microbiology* **68**, 177-194. (doi:10.1146/annurev-micro-091313-103654).

[6] Nussbaumer, A.D., Fisher, C.R. & Bright, M. 2006 Horizontal endosymbiont transmission in hydrothermal vent tubeworms. *Nature* **441**, 345-348. (doi:10.1038/nature04793).

[7] Laming, S.R., Gaudron, S.M. & Duperron, S. 2018 Lifecycle Ecology of Deep-Sea Chemosymbiotic Mussels: A Review. *Frontiers in Marine Science* **5**. (doi:10.3389/fmars.2018.00282).

[8] Fontanez, K.M. & Cavanaugh, C.M. 2014 Evidence for horizontal transmission from multilocus phylogeny of deep-sea mussel (*Mytilidae*) symbionts. *Environmental microbiology* **16**, 3608-3621. (doi:10.1111/1462-2920.12379).

[9] Won, Y.J., Hallam, S.J., O'Mullan, G.D., Pan, I.L., Buck, K.R. & Vrijenhoek, R.C. 2003 Environmental Acquisition of Thiotrophic Endosymbionts by Deep-Sea Mussels of the Genus *Bathymodiolus*. *Appl Environ Microbiol* **69**, 6785-6792. (doi:10.1128/aem.69.11.6785-6792.2003).

[10] Won, Y.J., Jones, W.J. & Vrijenhoek, R.C. 2008 Absence of cospeciation between deep-sea mytilids and their thiotrophic endosymbionts. *Journal of Shellfish Research* **27**, 129-138. (doi:10.2983/0730-8000(2008)27[129:AOCBDM]2.0.CO;2).

[11] Russell, S.L., Pepper, E., Svedberg, J., Byrne, A., Castillo, J.R., Vollmers, C., Beinart, R.A. & Corbett-Detig, R. 2019 Horizontal transmission and recombination maintain forever young bacterial symbiont genomes. *bioRxiv*, 754028. (doi:10.1101/754028).

[12] Wentrup, C., Wendeberg, A., Schimak, M., Borowski, C. & Dubilier, N. 2014 Forever competent: deep-sea bivalves are colonized by their chemosynthetic symbionts throughout their lifetime. *Environmental microbiology* **16**, 3699-3713. (doi:10.1111/1462-2920.12597).

[13] Arellano, S.M., Van Gaest, A.L., Johnson, S.B., Vrijenhoek, R.C. & Young, C.M. 2014 Larvae from deep-sea methane seeps disperse in surface waters. *Proceedings. Biological sciences* **281**, 20133276. (doi:10.1098/rspb.2013.3276).

[14] Arellano, S.M. & Young, C.M. 2009 Spawning, development, and the duration of larval life in a deep-sea cold-seep mussel. *Biol Bull* **216**, 149-162. (doi:10.1086/BBLv216n2p149).

[15] Salerno, J.L., Macko, S.A., Hallam, S.J., Bright, M., Won, Y.J., McKiness, Z. & Van Dover, C.L. 2005 Characterization of symbiont populations in life-history stages of mussels from chemosynthetic environments. *Biological Bullitin* **208**, 145-155. (doi:10.2307/3593123).

[16] Tyler, P.A. & Young, C.M. 1999 Reproduction and dispersal at vents and cold seeps. *Journal of the Marine Biological Association of the United Kingdom* **79**, 193-208. (doi:10.1017/S0025315499000235).

[17] Thubaut, J., Puillandre, N., Faure, B., Cruaud, C. & Samadi, S. 2013 The contrasted evolutionary fates of deep-sea chemosynthetic mussels (Bivalvia, Bathymodiolinae). *Ecology and evolution* **3**, 4748-4766. (doi:10.1002/ece3.749).

[18] Bayne, B.L. 1971 Some morphological changes that occur at the metamorphosis of the larvae of *Mytilus edulis*. In *The Fourth European Marine Biology Symposium* (pp. 259-280.

[19] Cannuel, R., Beninger, P.G., Mc Combie, H. & Boudry, P. 2009 Gill Development and Its Functional and Evolutionary Implications in the Blue Mussel *Mytilus edulis*. *Biolobical Bulletin* **217**, 173-188. (doi:10.1086/BBLv217n2p173).

[20] Montanaro, J., Gruber, D. & Leisch, N. 2016 Improved ultrastructure of marine invertebrates using non-toxic buffers. *PeerJ* **4**, e1860. (doi:10.7717/peerj.1860).

[21] Handschuh, S., Baeumler, N., Schwaha, T. & Ruthensteiner, B. 2013 A correlative approach for combining microCT light and transmission electron microscopy in a single 3D scenario. *Frontiers in Zoology* **10**. (doi:10.1186/1742-9994-10-44).

[22] Stoecker, K., Dorninger, C., Daims, H. & Wagner, M. 2010 Double labeling of oligonucleotide probes for fluorescence in situ hybridization (DOPE-FISH) improves signal intensity and increases rRNA accessibility. *Appl Environ Microbiol* **76**, 922-926. (doi:10.1128/AEM.02456-09).

[23] Wilde, F., Ogurreck, M., Greving, I., Hammel, J.U., Beckmann, F., Hipp, A., Lottermoser, L., Khokhriakov, I., Lytaev, P., Dose, T., et al. 2016 Micro-CT at the imaging beamline P05 at PETRA III. *AIP Conference Proceedings* **1741**, 030035. (doi:10.1063/1.4952858).

[24] Geier, B., Franke, M., Ruthensteiner, B., Porras, M.Á.G., Gruhl, A., Wörmer, L., Moosmann, J., Hammel, J.U., Dubilier, N., Leisch, N., et al. 2019 Correlative 3D anatomy and spatial chemistry in animal-microbe symbioses: developing sample preparation for phase-contrast synchrotron radiation based micro-computed tomography and mass spectrometry imaging. In *SPIE Optical Engineering + Applications* (eds. B. Müller & G. Wang), SPIE.

[25] van Aarle, W., Palenstijn, W.J., Cant, J., Janssens, E., Bleichrodt, F., Dabravolski, A., De Beenhouwer, J., Joost Batenburg, K. & Sijbers, J. 2016 Fast and flexible X-ray tomography using the ASTRA toolbox. *Opt. Express* **24**, 25129-25147. (doi:10.1364/oe.24.025129).

[26] van Aarle, W., Palenstijn, W.J., De Beenhouwer, J., Altantzis, T., Bals, S., Batenburg, K.J. & Sijbers, J. 2015 The ASTRA Toolbox: A platform for advanced algorithm development in electron tomography. *Ultramicroscopy* **157**, 35-47. (doi:10.1016/j.ultramic.2015.05.002).

[27] Moosmann, J., Ershov, A., Weinhardt, V., Baumbach, T., Prasad, M.S., LaBonne, C., Xiao, X., Kashef, J. & Hofmann, R. 2014 Time-lapse X-ray phase-contrast microtomography for in vivo imaging and analysis of morphogenesis. *Nature Protocols* **9**, 294. (doi:10.1038/nprot.2014.033).

[28] Cardona, A., Saalfeld, S., Schindelin, J., Arganda-Carreras, I., Preibisch, S., Longair, M., Tomancak, P., Hartenstein, V. & Douglas, R.J. 2012 TrakEM2 Software for Neural Circuit Reconstruction. *PloS one* **7**, e38011. (doi:10.1371/journal.pone.0038011).

[29] Fisher, C.R., Childress, J.J., Oremland, R.S. & Bidigare, R.R. 1987 The importance of methane and thiosulfate in the metabolism of the bacterial symbionts of two deep-sea mussels. *Marine Biology* **96**, 59-71. (doi:10.1007/BF00394838).

[30] Bayne, B.L. 1965 Growth and the delay of metamorphosis of the larvae of M*ytilus edulis* (L.).

Ophelia **2**, 1-47. (doi:10.1080/00785326.1965.10409596).

[31] Gallager, S.M., Mann, R. & Sasaki, G.C. 1986 Lipid as an index of growth and viability in three species of bivalve larvae. *Aquaculture* **56**, 81-103. (doi:10.1016/0044-8486(86)90020-7).

[32] Breusing, C., Biastoch, A., Drews, A., Metaxas, A., Jollivet, D., Vrijenhoek, R.C., Bayer, T., Melzner, F., Sayavedra, L., Petersen, J.M., et al. 2016 Biophysical and Population Genetic Models Predict the Presence of "Phantom" Stepping Stones Connecting Mid-Atlantic Ridge Vent Ecosystems. *Current biology : CB* **26**, 2257-2267. (doi:10.1016/j.cub.2016.06.062).

[33] Distel, D.L., Baco, A.R., Chuang, E., Morrill, W., Cavanaugh, C. & Smith, C.R. 2000 Do mussels take wooden steps to deep-sea vents? *Nature* **403**, 725-726. (doi:10.1038/35001667).

[34] Kaper, J.B., Nataro, J.P. & Mobley, H.L.T. 2004 Pathogenic Escherichia coli. *Nature Reviews Microbiology* **2**, 123-140. (doi:10.1038/nrmicro818).

[35] Quarmby, L.M. 2004 Cellular Deflagellation. In *International Review of Cytology* (pp. 47-91, Academic Press.

[36] Tubiash, H.S., Chanley, P.E. & Leifson, E. 1965 Bacillary Necrosis, a Disease of Larval and Juvenile Bivalve Mollusks I. Etiology and Epizootiology. *Journal of Bacteriology* **90**, 1036.

[37] Le Pennec, M., Benninger, P.G. & Herry, A. 1995 Feeding and digestive adaptations of bivalve molluscs to sulphide-rich habitats. *Comparative Biochemistry and Physiology* **111**, 183-189. (doi:10.1016/0300-9629(94)00211-B).

[38] Von Cosel, R., Comtet, T. & Krylova, E.M. 1999 *Bathymodiolus* (Bivalvia: *Mytilidae*) from Hydrothermal Vents on the Azores Triple Junction and the Logatchev Hydrothermal Field, Mid-Atlantic Ridge. *The Veliger* **42**, 218-248.

[39] Karasov, W.H. & Douglas, A.E. 2013 Comparative digestive physiology. *Compr Physiol* **3**, 741-783. (doi:10.1002/cphy.c110054).

[40] Von Cosel, R. & Marshall, B.A. 2010 A new genus and species of large mussel (Mollusca: Bivalvia: *Mytilidae*) from the Kermadec Ridge. *Records of the Musuem of NEw Zwaland Te Papa* **21**, 15.

[41] Eckelbarger, K.J. & Young, C.M. 1999 Ultrastructure of gametogenesis in a chemosynthetic mytilid bivalve (Bathymodiolus childressi) from a bathyal, methane seep environment (northern Gulf of Mexico). *Marine Biology* **135**, 635-646. (doi:10.1007/s002270050664).

[42] Le Pennec, M. & Beninger, P. 1997 Aspects of the reproductive strategy of bivalves from reducing-ecosystem. *Cah. Biol. Mar* **38**, 132-133.

[43] Laming, S.R., Duperron, S., Gaudron, S.M., Hilario, A. & Cunha, M.R. 2015 Adapted to change: The rapid development of symbiosis in newly settled, fast-maturing chemosymbiotic mussels in the deep sea. *Marine environmental research* **112**, 100-112. (doi:10.1016/j.marenvres.2015.07.014).

[44] Shikuma, N.J., Pilhofer, M., Weiss, G.L., Hadfield, M.G., Jensen, G.J. & Newman, D.K. 2014 Marine Tubeworm Metamorphosis Induced by Arrays of Bacterial Phage Tail–Like Structures. *Science* **343**, 529. (doi:10.1126/science.1246794).

[45] Desbruyères, D., Almeida, A., Biscoito, M., Comtet, T., Khripounoff, A., Le Bris, N., Sarradin, P.M. & Segonzac, M. 2000 A review of the distribution of hydrothermal vent communities along the northern Mid-Atlantic Ridge: dispersal vs. environmental controls. In *Island, Ocean and Deep-Sea Biology* (eds. M.B. Jones, J.M.N. Azevedo, A.I. Neto, A.C. Costa & A.M.F. Martins), pp. 201-216. Dordrecht, Springer Netherlands.

[46] Ansorge, R., Romano, S., Sayavedra, L., Porras, M.Á.G., Kupczok, A., Tegetmeyer, H.E., Dubilier, N. & Petersen, J. 2019 Functional diversity enables multiple symbiont strains to coexist in deep-sea mussels. *Nature microbiology* **4**, 2487-2497. (doi:10.1038/s41564-019-0572-9).

[47] Wentrup, C., Wendeberg, A., Huang, J.Y., Borowski, C. & Dubilier, N. 2013 Shift from widespread symbiont infection of host tissues to specific colonization of gills in juvenile deep-sea mussels. *The ISME journal* **7**, 1244-1247. (doi:10.1038/ismej.2013.5).

[48] Streams, M.E., Fisher, C.R. & Fiala-Médioni, A. 1997 Methanotrophic symbiont location and fate of carbon incorporated from methne in a hydrocabon seep mussel. *Marine Biology* **129**, 465-476. (doi:10.1007/s002270050187).

[49] Nyholm, S.V. & Graf, J. 2012 Knowing your friends: invertebrate innate immunity fosters beneficial bacterial symbioses. *Nature Reviews Microbiology* **10**, 815-827. (doi:10.1038/nrmicro2894).

[50] Zheng, P., Wang, M., Li, C., Sun, X., Wang, X., Sun, Y. & Sun, S. 2017 Insights into deep-sea adaptations and host–symbiont interactions: A comparative transcriptome study on *Bathymodiolus* mussels and their coastal relatives. *Molecular ecology* **26**, 5133-5148. (doi:10.1111/mec.14160).

[51] Wong, Y.H., Sun, J., He, L.S., Chen, L.G., Qiu, J.-W. & Qian, P.-Y. 2015 High-throughput transcriptome sequencing of the cold seep mussel *Bathymodiolus platifrons*. *Sci Rep* **5**, 16597-16611. (doi:10.1038/srep16597).

[52] Sun, J., Zhang, Y., Xu, T., Zhang, Y., Mu, H., Zhang, Y., Lan, Y., Fields, C.J., Hui, J.H.L., Zhang, W., et al. 2017 Adaptation to deep-sea chemosynthetic environments as revealed by mussel genomes. *Nat Ecol Evol* **1**, 121. (doi:10.1038/s41559-017-0121).